

Combination of crystal growth with optical floating zone and evaluation of $\text{Nd}^{3+}:\text{LaAlO}_3$ crystals with the dynamic nuclear polarization of ^{139}La and ^{27}Al

Kohei Ishizaki¹, Ikuo Ide¹, Masaki Fujita², Hiroki Hotta¹, Yuki Ito¹, Masataka Inuma³, Yoichi Ikeda², Takahiro Iwata⁴, Masaaki Kitaguchi⁵, Hideki Kohri^{6,1}, Taku Matsushita¹, Daisuke Miura⁴, Yoshiyuki Miyachi⁴, Hirohiko M. Shimizu¹, and Masaru Yosoi⁶

¹*Nagoya University, Furocho, Chikusa, Nagoya, 464-8602, Japan*

²*Institute for Materials Research, Tohoku University, Sendai 980-8577, Japan*

³*Hiroshima University, Kagamiyama, Higashi-hiroshima, 739-8527, Japan*

⁴*Yamagata University, Koshirakawa, Yamagata 990-8560, Japan*

⁵*KMI, Nagoya University, Furocho, Chikusa, Nagoya, 464-8602, Japan*

⁶*Research Center for Nuclear Physics, Osaka University, Ibaraki, Osaka, 567-0047, Japan*

(*Electronic mail: ishizaki@phi.phys.nagoya-u.ac.jp)

(Dated: 2 May 2024)

Producing a polarized lanthanum (La) target with high polarization and long relaxation time is crucial for realizing time-reversal violation experiments using polarized neutron beams. We use a LaAlO_3 crystal doped with a small amount of Nd^{3+} ions for the polarized lanthanum target. Optimizing the amount of Nd^{3+} ions is considerably important because the achievable polarization and relaxation time strongly depend on this amount. We established a fundamental method to grow single crystals of $\text{Nd}^{3+}:\text{LaAlO}_3$ using an optical floating zone method that employs halogen lamps and evaluated the crystals with the dynamic nuclear polarization (DNP) method for polarizing nuclear spins. Two crystal samples were grown by ourselves and evaluated with the DNP at 1.3 K and 2.3 T for the first time except for the target materials of protons. The enhancement of NMR signals for ^{139}La and ^{27}Al was successfully observed, and the enhancement factors were eventually 3.5 ± 0.3 and 13 ± 3 for the samples with Nd^{3+} ions of 0.05 and 0.01 mol%, respectively. These enhancement factors correspond to absolute vector polarizations of $0.27 \pm 0.02\%$ (Nd^{3+} 0.05 mol%) and $1.4 \pm 0.3\%$ (Nd^{3+} 0.01 mol%). Although the obtained polarizations are still low, they are acceptable as a first step. The combination scheme of the crystal growth and evaluation of the crystals is found to be effectively applicable for optimizing the amount of Nd^{3+} ions for improving the performance of the polarized target.

I. INTRODUCTION

Wu et al. first found the violation of discrete symmetry in a nucleus via polarized ^{60}Co experiments¹. Similar parity non-conservation effects in nuclei were observed in the polarized neutron scattering with the unpolarized nuclei. Many types of nuclei, including lanthanum(^{139}La), showed large asymmetry in the absorption cross sections of a polarized neutron. The parity-violating asymmetry was enhanced to approximately $10^2 - 10^6$ times larger than that of the proton-proton scattering². The asymmetry can be explained by both the multi-body effect in the nucleus and the interference between the large parity-conserving scattering amplitude and tiny parity-nonconserving one². Theoretical studies predicted similar enhancements in the time-reversal violating interaction for certain nuclei³. Recent experimental results showed that ^{139}La is a promising target for exploring the enhancement-assisted T-violation effects^{4,5}.

One difficulty in the T-violation experiment is realizing the polarized ^{139}La target. One possible method to achieve high polarization is dynamic nuclear polarization (DNP) with a LaAlO_3 crystal, where a small amount of La^{3+} ions are replaced with Nd^{3+} ions behaving as a paramagnetic dopant in the DNP⁶. In the past, two DNP experiments reported the enhancement of the vector polarization of ^{139}La in the $\text{Nd}^{3+}:\text{LaAlO}_3$ crystal with Nd 0.03 mol%. The vector polarization P_V is defined as

$$P_V = \frac{\sum_{m=-I}^{m=+I} m P_m}{I \sum_{m=-I}^{m=+I} P_m}, \quad (1)$$

where I represents a nuclear spin, m represents a spin quantum number, P_m represents the population on state m of the target nuclear spins. Hereafter, the vector polarization is expressed as "polarization". The first experiment was conducted at approximately 1.5 K and 2.3 T⁷, and the polarization of 0.2 for ^{139}La was achieved. In another experiment, polarizations of 0.62 and 0.475 for ^{27}Al and ^{139}La in the Nd 0.03 mol% crystal were obtained using a dilution refrigerator at 2.3 T⁸. These results show the potentiality of the $\text{Nd}^{3+}:\text{LaAlO}_3$ crystal as the polarized target.

In the DNP, a dominant relaxation process of nuclear spins is caused by the magnetic fluctuation of paramagnetic ions, which are coupled to nuclear spins via the dipole-dipole interaction. Hence, such relaxation effects can be suppressed by reducing the Nd^{3+} amount. However, it reduces the efficiency of polarization transfer from the electron polarization to nuclear spins. For increasing polarization, it is necessary to determine the optimal Nd^{3+} amount by studying the relationship between Nd^{3+} concentration and polarization enhancement. Establishing a fundamental method for growing the crystal samples by ourselves is preferred because it allows us to flexibly prepare

various samples with different Nd^{3+} amounts.

LaAlO_3 crystals are usually produced via the Czochralski method^{9,10}. The Bridgman method is also applicable to the growth of the LaAlO_3 crystals¹¹. These methods are suited for growing large crystals; however, they are too costly to flexibly prepare several appropriate crystals required for studying fundamental properties. In addition, the precise control of unexpected impurities and the required Nd^{3+} amounts are difficult because some procedures with a crucible are unavoidable in these methods. In contrast, an optical floating zone (FZ) method is applicable for growing a good-sized sample at a low cost. The properties of the LaAlO_3 crystals are low optical absorption and high melting point (2100 °C), and therefore, to the best of our knowledge regarding the optical FZ method, there are no reports of growing LaAlO_3 crystals except for melting by xenon lamps^{12–14}. Instead of the xenon lamps, we attempted to grow a crystal without any dopant and a crystal with Nd^{3+} 0.05 mol% using halogen lamps¹⁵ although an achievable temperature was comparable to the melting point. One benefit of the latter method is that a generalized apparatus is available, which is more versatile and inexpensive than the former. The effectiveness of this approach can be verified by performing simple DNP experiments.

In this paper, we present the first confirmation regarding the effectiveness of the optical FZ method using halogen lamps and the first results of the DNP experiments of $\text{Nd}^{3+}:\text{LaAlO}_3$ crystals produced by ourselves with the DNP at 1.3 K and 2.3 T. The rest of the paper is organized as follows. In section 2, we focus on the importance and motivation of the combination scheme of the crystal growth and the evaluation with DNP. Section 3 explains the crystal growth with the FZ method using halogen lamps. Section 3 also shows the experimental results of the DNP experiments with two types of crystal samples prepared with the optical FZ method. Finally, section 4 summarizes the results and presents the future prospects.

II. PROCEDURE OF CRYSTAL GROWTH AND EVALUATION OF CRYSTALS

The achievable polarization and relaxation time are strongly dependent on the amount of Nd^{3+} ions in a LaAlO_3 crystal, and therefore, many cycles of crystal growth and evaluations are required to optimize the amount of Nd^{3+} ions. Figure 1 shows the procedures of a cycle. Some LaAlO_3 crystals with different amounts of Nd^{3+} ions are grown in the first step. The crystals are cooled at ~ 1.5 K, and DNP is performed using microwaves at a magnetic field of a few Tesla in the second step. The polarizations and relaxation times are obtained by data analysis in the third step.

Feedback from the results of the data analysis improves the next cycle, and the cycles are repeated until the optimal amount of the Nd^{3+} ions is determined. A fundamental approach for growing the crystals needs to be established to perform a cycle, which is sufficiently effective for the DNP, with precise control of the Nd amount in the range of 0.01 mol%. Furthermore, it is desirable for the DNP system to be simple and easy to use for implementing flexible and rapid DNP tests. The first issue for moving the cycle into action is to check the control of the Nd amount in the crystal growth. Therefore, it is necessary to grow two crystals with different Nd amount and to confirm whether their difference can be observed in the DNP evaluation.

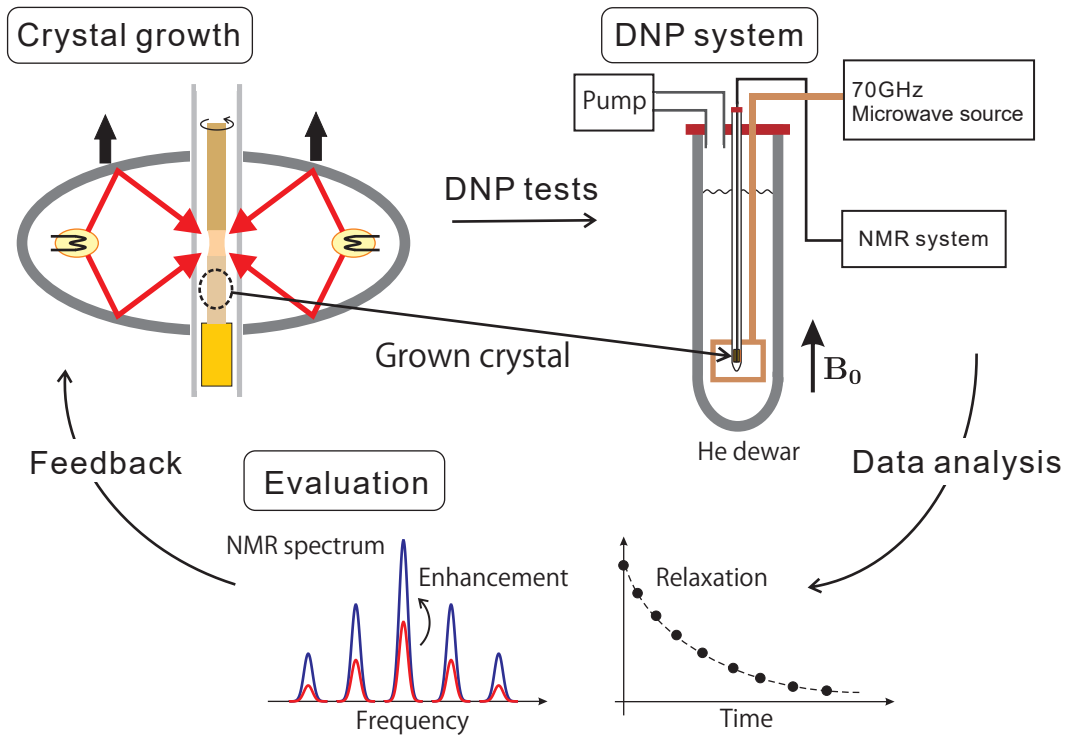


FIG. 1. Combination scheme of the crystal growth and evaluation of crystals with the DNP.

III. CRYSTAL GROWTH USING FLOATING ZONE METHOD

A. Structure of LaAlO_3 crystals

The crystal structure of LaAlO_3 and its dependence on the temperature have been studied using neutron powder diffraction¹⁶. Above 813 K, the crystal structure is perovskite, whereas a distorted-perovskite structure appears below 813 K, and the unit cell only has a threefold rotation (C_3) axis.

Even in the structure below 813 K, all La and Al sites are magnetically equivalent and have uniaxial magnetic symmetry, respectively. The distortion is so tiny that LaAlO_3 crystals spontaneously form twin domains in the structural phase transition. All domains in the crystal are assorted into four groups according to the direction of the C_3 axis. In the DNP experiments, the crystal samples must be aligned so that the C_3 axis of one domain becomes parallel to the external magnetic field. In this paper, the domain with the C_3 axis parallel to the external magnetic field is referred to as the "primary domain", and the other domains are the "secondary domain" .

B. Crystal growth

The details of our crystal growth method using halogen lamps have been explained elsewhere¹⁵. Here, we present a brief summary. The raw materials were $\text{La}(\text{OH})_3$ (4N), Al_2O_3 (4N), and Nd_2O_3 (3N). Each powder of LaAlO_3 and $\text{La}_{0.99}\text{Nd}_{0.01}\text{AlO}_3$ was synthesized by mixing the raw materials according to the stoichiometric ratio and calcining at 1400 °C for over 8 h. The powder of $\text{Nd}^{3+}:\text{LaAlO}_3$ with Nd 0.05 mol% or 0.01 mol% was prepared by mixing LaAlO_3 and $\text{La}_{0.99}\text{Nd}_{0.01}\text{AlO}_3$. The feed and seed rods were shaped by cold isostatic pressing and sintering them at 1400 °C for over 8 h. The seed crystal was placed on the seed rod to grow the crystal along the C_3 axis. As shown in Fig. 2, the feed rod and seed crystal were melded by converging the infrared ray in the FZ furnace (Crystal Systems Co.), which consisted of four 1 kW halogen lamps. The optimal condition for growing was 10 mm/h in the air. Samples were successfully grown to lengths ranging from 10-20 mm and diameters of ~ 5 mm, which is suitable for developing polarized targets.

For the DNP experiments, we prepared two crystal samples with Nd 0.05 and 0.01 mol%. The former was dark brown and the latter was light brown. Although the reason of such a difference of color is not specified yet, the problem is expected to be resolved by repeating the cycle shown in Fig. 1. At this time, therefore, it is important to directly compare the results of the DNP between these crystals.

C. Selection of grown crystals with EPR and NMR

We confirmed that the grown samples had a single crystal and that the growth direction corresponded to the C_3 axis in the cubic phase using the X-ray Laue technique. In the next step, the

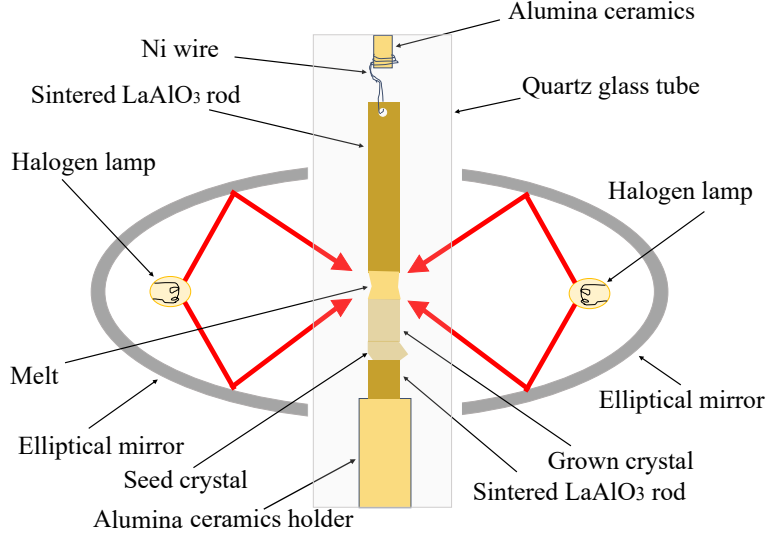


FIG. 2. Schematic of the FZ apparatus used for crystal growth. The FZ apparatus is equipped with four halogen lamps, but only two mirrors are drawn for clarity.

electron paramagnetic resonance (EPR) of Nd^{3+} ions in the 0.05 mol% sample was measured at 10 K using the CW-EPR with a 9.5 GHz microwave. The effective g -factor and EPR linewidth at full-width-half maximum in the primary domain were obtained as 2.12 and 6 G, respectively. These values were comparable to those in the LaAlO_3 sample used in the previous experiments^{6,15}. The linewidth is attributed to the super-hyperfine interaction between the ^{27}Al nucleus and Nd^{3+} ions⁶.

The EPR measurement revealed that the volume of the domain with the C_3 axis parallel to the growth direction was small in the sample with Nd 0.05 mol%. We measured NMR spectra at 300 K and 6.9 T using a conventional pulse-NMR system. The direction of the C_3 axis of the largest domain was identified by changing orientation of the crystal. DNP experiments can be performed when the magnetic field is applied to the C_3 axis of the largest domain.

The frequency of the transition $m \leftrightarrow m + 1$ of the nuclear spin with $I(> 1/2)$ in the uniaxial electrical field gradient such as ^{139}La ($I = 7/2$) and ^{27}Al ($I = 5/2$) in LaAlO_3 is expressed as

$$v_{m \leftrightarrow m+1} = v_L - v_Q \left(\frac{3 \cos^2 \theta - 1}{2} \right) \left(m + \frac{1}{2} \right), \quad (2)$$

where v_L , v_Q , and θ represent the Larmor frequency of the nucleus, frequency shift parameter derived from the nuclear quadrupole interaction, and angle between the external magnetic field and symmetrical axis of the electric-field gradient, which corresponds to the C_3 axis in the domains⁸.

ν_Q depends on the sample temperature because the lattice parameters depend on the temperature. Further, each frequency shift parameter ν_Q for ^{27}Al in LaAlO_3 is +22 kHz and +30 kHz at 300 K and 1.3 K, respectively, whereas that for ^{139}La is +495 kHz and +673 kHz at 300 K and 1.3 K, respectively. The absolute value of ν_Q was measured in our experiments, and the sign was determined from the previous experiments⁸.

The angle between the C_3 axis of the secondary domains and external magnetic field is approximately 70° . The frequency shift induced by the nuclear quadrupole interaction in the secondary domains is one-third of that in the primary domain. In the NMR spectrum, the central frequency of each peak distinguishes between the primary or secondary domain using Eq. (2). The evaluation of the area of peaks leads to the ratio of the domain's volume in the sample.

IV. EVALUATION OF CRYSTALS WITH THE DNP METHOD

A. DNP apparatus

Figure 3 shows the apparatuses of two DNP experiments for crystal samples with Nd 0.05 and 0.01 mol%. The samples inside the sample box drawn in Fig. 3 (b-1) or (c-1) were cooled down to 1.3 K by pumping liquid ^4He in the glass dewar, as shown in Fig. 3 (a). The space between the inner and outer layers of the dewar was maintained as a vacuum to ensure thermal insulation. The outer layer was cooled by liquid nitrogen to reduce the consumption of liquid ^4He . The temperature was monitored with a ruthenium oxide thermometer and a platinum resistance thermometer attached to a brass box where the sample was installed.

In the first DNP experiment, the sample with Nd 0.05 mol% was fixed on the base plate made of ABS resin, which was produced with a 3D printer, as shown in Fig. 3 (b-1). We created a tiny cut in the sample as shown in Fig. 3 (b-2) to recognize the direction of the C_3 axis of the largest domain. The sample was fixed so that the tiny cut was in contact with the ABS resin, and the C_3 axis of the largest domain became parallel to the external magnetic field B_0 . The sample was directly cooled through thermal contact to the liquid ^4He .

In the second DNP experiment, we used a column-shaped sample with Nd 0.01 mol%, which was 4 mm in diameter and 5 mm in length, as shown in Fig. 3 (c-1, c-2). The sample was aligned such that the growth direction was parallel to the external magnetic field B_0 and placed in the quartz tube filled with ^4He gas. The sample temperature was decreased by cooling the quartz tube

with the liquid ^4He .

Microwaves with a frequency of ~ 70 GHz were generated using the microwave oscillator (ELVA-1 Ltd., VCOM-12) and guided into the brass box through a waveguide. The continuous wave NMR system with a Liverpool Q-meter was used to measure the enhancement of the polarization by sweeping the RF frequency¹⁷. As shown in Fig. 3(b-2, c-2), the NMR coils were wound on the samples. In the case of the sample with Nd 0.05 mol% (Fig. 3(b-2)), the NMR RF field was tilted by 20° from the perpendicular angle of the external magnetic field B_0 . It is noted that a reduction of the NMR sensitivity due to the tilted coil is estimated to be about 10%.

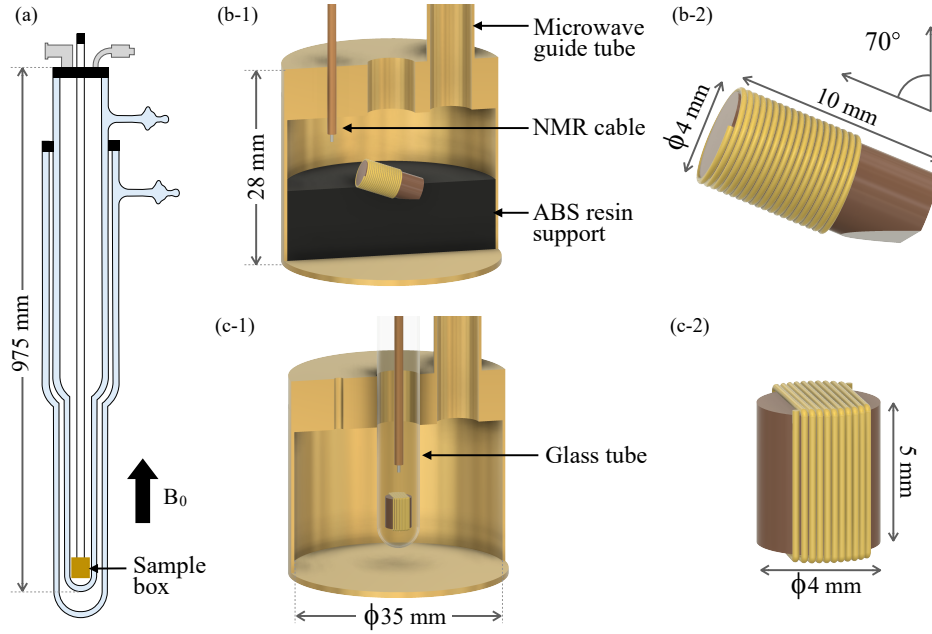


FIG. 3. Apparatuses of two DNP experiments for crystal samples with (a) liquid He dewar, (b-1) sample box of Nd 0.05 mol%, and (c-1) sample box of Nd 0.01 mol%. The NMR coils and LaAlO_3 crystal samples with Nd (b-2) 0.05 and (c-2) 0.01 mol%.

B. NMR measurements

We calculate the NMR peak shift $\Delta\nu_m$ from the peak of the $-1/2 \leftrightarrow +1/2$ transition using

$$\Delta\nu_m = \nu_{m \leftrightarrow m+1} - \nu_{-1/2 \leftrightarrow +1/2}. \quad (3)$$

The calculated $\Delta\nu_m$ for ^{27}Al is listed in Table I.

TABLE I. NMR peak assignment and peak shift $\Delta\nu_{m \leftrightarrow m+1}$ for ^{27}Al in the primary (p) and secondary (s) domains at 1.3 K.

Peak index	$m \leftrightarrow m+1$	$\Delta\nu_m$ [kHz]	domain
(1)	$+3/2 \leftrightarrow +5/2$	-60	p
(2)	$+1/2 \leftrightarrow +3/2$	-30	p
(3)	$-5/2 \leftrightarrow -3/2$	-20	s
(4)	$-3/2 \leftrightarrow -1/2$	-10	s
(5)	$-1/2 \leftrightarrow +1/2$	0	p+s
(6)	$+1/2 \leftrightarrow +3/2$	10	s
(7)	$+3/2 \leftrightarrow +5/2$	20	s
(8)	$-3/2 \leftrightarrow -1/2$	30	p
(9)	$-5/2 \leftrightarrow -3/2$	60	p

As indicated in Table I, the two peak intensities of the primary and secondary domains are mixed in the transition of $-1/2 \leftrightarrow +1/2$ because of the lack of an anisotropic aspect. The microwave frequency was tuned to enhance the NMR peaks of the primary domain. We used the peak intensities of the $+1/2 \leftrightarrow +3/2$ (peak (2)) and $-3/2 \leftrightarrow -1/2$ (peak (8)) transitions to evaluate the enhancement of the ^{27}Al polarization for the samples with Nd 0.05 mol% and 0.01 mol%, respectively, because the peaks were attributed only to the primary domain and were easily identified in the ^{27}Al -NMR spectrum. All NMR peaks were within a sweep range of the RF frequency, ~ 0.2 MHz, which was determined by the Q curve. In contrast, only one NMR peak was observed for ^{139}La in a sweep range because of the large quadrupole interaction. For evaluating the enhancement of the ^{139}La polarization, we observed the center peak corresponding to the $-1/2 \leftrightarrow +1/2$ transition. NMR signals were measured at 1.3 K and 4.2 K, and baseline shifts attributed to different cooling condition were not observed. The sensitivity of NMR measurements was inferred to be unchanged.

C. Enhancement of the ^{139}La and ^{27}Al polarizations with the Nd 0.05 mol% sample

Figure 4 shows two ^{139}La -NMR spectra, where one was measured after a sufficiently long time of microwave irradiation, and the other was obtained at the thermal equilibrium(TE) state at 1.3 K

and 2.3 T. The peak of the $-1/2 \leftrightarrow +1/2$ transition is clearly observed and a small enhancement of the ^{139}La polarization is successfully observed.

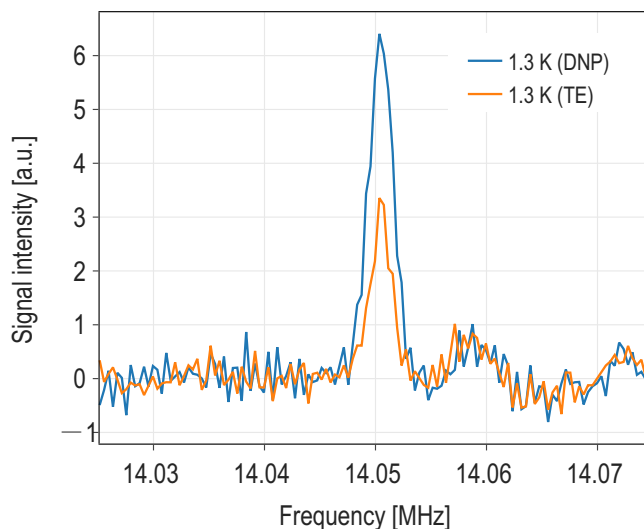


FIG. 4. ^{139}La -NMR spectra of the $-1/2 \leftrightarrow +1/2$ transition with the Nd 0.05 mol% sample at 1.3 K and 2.3 T.

Figure 5 (a) shows the build-up curve of the ^{139}La polarization after inputting microwaves with a frequency of 69.345 GHz. The build-up time is obtained as 10 ± 2 min by fitting the curve with an exponential function. If the contribution of the secondary domain is ignored, the $-1/2 \leftrightarrow +1/2$ signal after inputting the microwaves becomes 2.3 ± 0.2 times larger than that at the TE state.

After turning off the microwaves, the NMR peak intensity became smaller and was closer to that at the TE state, as shown in Fig. 5 (b). The decay curve of the polarization is fitted with an exponential function, and the relaxation time of the polarization is obtained as 19 ± 2 min. The build-up time is roughly two times shorter than the relaxation time.

The results of ^{27}Al under the same condition reveal two NMR spectra at the TE and saturated states, as shown in Fig. 6. Seven peaks are clearly observed at both states, and additional two structures, indicated as (3) and (7), are also observed. The peak assignment is shown in Table I. The peak intensity of the $+1/2 \leftrightarrow +3/2$ transition becomes 2.5 ± 0.2 times larger than that measured at the TE state. This enhancement corresponds to an absolute vector polarization of $0.28 \pm 0.02\%$. The uncertainties are mostly due to the fluctuation of the baselines under the NMR peaks. Further, only peaks of the primary domain were enhanced by the irradiation of the microwaves, and the peaks of the secondary domain were unchanged. This implies that the microwave frequency was well tuned to the primary domain. The NMR spectrum at the TE state provides the volume

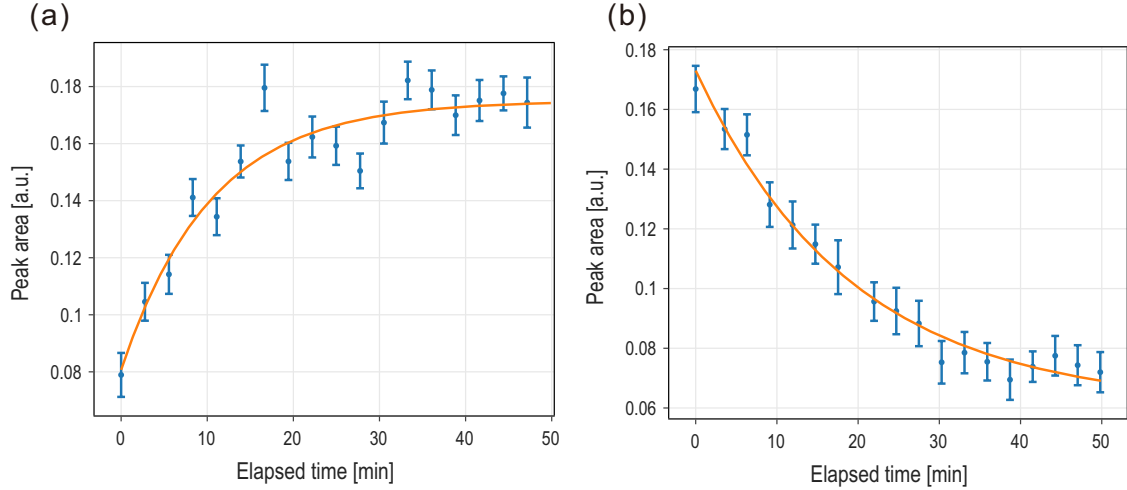


FIG. 5. (a) Time dependence of the peak area of the $-1/2 \leftrightarrow +1/2$ transition in ^{139}La -NMR (Nd 0.05 mol%) after inputting the 69.345 GHz microwaves. (b) Time dependence of the peak area of the $-1/2 \leftrightarrow +1/2$ transition in ^{139}La -NMR (Nd 0.05 mol%) after turning off the microwaves.

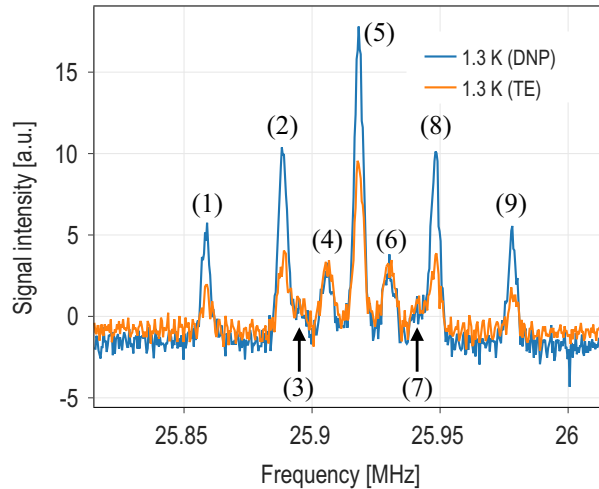


FIG. 6. ^{27}Al -NMR spectrum of the sample with Nd 0.05 mol% at 2.3 T. The indices (1), ..., (9) represent peak index referred in Table I.

information of the domains in the sample with Nd 0.05 mol%. The ^{27}Al -NMR intensity of the peak (6) is nearly equal to that of the peak (2) at the TE state in Fig. 6. These peaks are for the $+1/2 \leftrightarrow +3/2$ transition, and the peak (6) and peak (2) are in the secondary and primary domains, respectively, as shown in Table I. This is also the case for the (4) and (8) peaks. The volumes of the primary and secondary domains are inferred to be nearly equal.

The results of ^{27}Al indicate that the presence of the secondary domains does not affect the enhancement in the primary domain. We assume that only the component of the primary domain is enhanced regardless of the presence of the secondary domain. Although the $-1/2 \leftrightarrow +1/2$ peak at the TE state contains the contribution of both primary and secondary domains, the assumption allows us to estimate the peak intensity of only the primary domain in the ^{139}La -NMR spectrum at the TE state. If equal volumes of the primary and secondary domains are assumed, the enhancement for ^{139}La at the saturated state is estimated to be 3.5 ± 0.3 which corresponds an absolute vector polarization of $0.27 \pm 0.02\%$. The uncertainties are mostly due to the fluctuation of the baselines under the NMR peaks.

D. Enhancement of the ^{27}Al polarization with the Nd 0.01 mol% sample

The spin temperature of ^{139}La is estimated to be approximately equal to that of ^{27}Al at all times. Considering that the observation of the ^{27}Al -NMR is considerably easier than that of ^{139}La -NMR, the ^{27}Al signals are very useful as an indicator for comparing two samples with Nd 0.05 and 0.01 mol%.

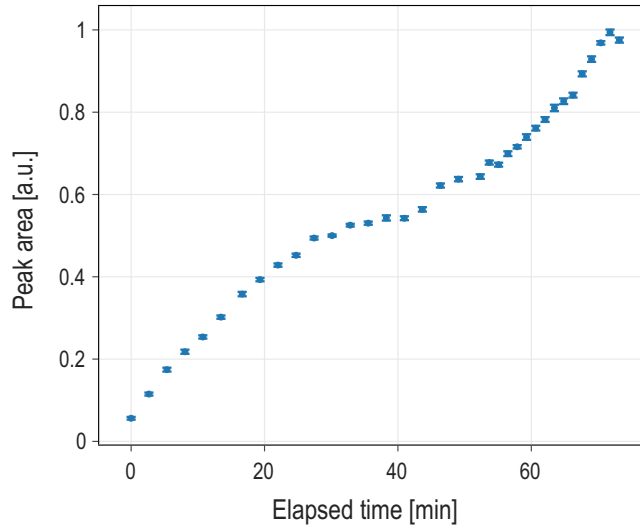


FIG. 7. The time dependence of the area of the ^{27}Al -NMR peak (peak (8) in Table I) during the irradiation of microwaves with frequencies of about 69.3 GHz. The frequencies were tuned three times between 40 and 70 min.

Figure 7 shows that the ^{27}Al polarization grew after inputting microwaves. The polarization growth was saturated once between the elapsed times of 30 and 40 min, and the growth restarted

around 40 min and continued until 70 min. The frequencies of the microwaves were changed at 40, 55, 63 min between 69.345 and 69.360 GHz. As a result, the time dependence of the peak area became different from a typical build-up curve. The measurement time was limited by the amount of liquid ^4He stored in the dewar, which was not equipped with a system that could supply liquid ^4He continuously. Although the polarization growth is not saturated, this result implies that the relaxation time of the ^{27}Al polarization at 1.3 K and 2.3 T is longer than 70 min. The observation of the TE NMR peaks at 1.3 K was difficult because of the limitation of time for leaving the sample. Thus, we measured the intensity of the TE signal at 4.2 K with an accuracy of 22% and estimated the intensity at 1.3 K by multiplying with a factor of 3.23(=4.2/1.3). The intensity of the NMR signal after the DNP was measured with an accuracy of 5%. Although the ^{27}Al polarization growth is not saturated, the maximum enhancement at 1.3 K results in 13 ± 3 which corresponds to an absolute vector polarization of $1.4 \pm 0.3\%$. The uncertainties are mostly due to the fluctuation of the baselines under the NMR peaks. Therefore, the enhancement with the Nd 0.01 mol% sample is at least 5 times larger than that with the Nd 0.05 mol% sample, although their experimental setups are not exactly identical.

V. SUMMARY AND FUTURE PROSPECTS

We grew two LaAlO_3 crystals with Nd 0.05 and 0.01 mol%, and performed the first DNP experiment at 1.3 K and 2.3 T. We succeeded in observing the enhancement of NMR signals for ^{139}La and ^{27}Al . The DNP for positive nuclear polarizations was performed, and that for negative polarization was not attempted. For the sample with Nd 0.05 mol%, we observed an enhancement of 3.5 ± 0.3 for ^{139}La . The result of the 0.01 mol% sample showed that the enhancement for ^{27}Al was ~ 5 times larger than that of the 0.05 mol% sample, although the experimental setups were not completely identical. These enhancements correspond to absolute vector polarizations of $0.27 \pm 0.02\%$ (Nd 0.05 mol%) and $1.4 \pm 0.3\%$ (Nd 0.01 mol%). The experimental results and comparison with the previous result of Nd 0.03 mol% confirm that our method can provide samples that are sufficiently effective for DNP. Further, a Nd concentration less than 0.03 mol% was found to be suitable for improving the polarization of the polarized target.

The size of the polarized target for the T-violation experiment is a few 10 times larger than that of the present crystal samples. However, it is difficult to grow such a large crystal with the optical FZ method. One possibility is to apply another method, which can grow larger LaAlO_3

crystals, with a crucible. Contamination deteriorating the performance of the polarized target must be removed from the crucible. The microwave heat generated in the crystal is accumulated in the large crystal. The heat conductivity of the LaAlO_3 crystal is too small to sufficiently cool the inside of the crystal from the surface at a low temperature. Dividing the crystal into some pieces can be a good way for the cooling. Another possibility is to grow many crystals with the same size as the present ones using the optical FZ method, and to combine them as a target. The C_3 axes of all crystals are aligned to the external magnetic field, and therefore, special treatments are required for the installation and cooling of the crystals.

The relaxation times of the polarizations were not measured in the present experiment because a one-shot cryostat was used. The temperature of 1.3 K lasted for only 6 h in which the relaxation time could not be measured precisely after the build-up of the polarization. Currently, we are developing a new cryostat that is operated continuously by filling it with liquid helium. The new cryostat has a needle valve that produces the pressure difference between the sample space and liquid helium bath. A relaxation time longer than 1 day will be measured in the near future.

Toward the realization of the polarized ^{139}La target, we established the primary method for growing LaAlO_3 crystals doped with Nd^{3+} ions with the optical FZ method using halogen lamps and evaluating the crystals with the DNP. This is expected to play a critical role in finding the optimal amount of Nd^{3+} ions to obtain a higher polarization and a longer relaxation time of the polarization. In fact, our recent experiment with a Nd^{3+} 0.01 mol% sample achieved a larger enhancement for the ^{139}La -NMR peak¹⁸. Most established polarized targets have been limited to proton and deuteron targets. Our positive results in the development of the polarized lanthanum target are unique in the nuclear and particle physics field. We hope the present method for target development will be used for not only the lanthanum targets but also for various nuclear targets in the future.

VI. AUTHOR DECLARATIONS

Conflict of Interest

The authors have no conflicts to disclose.

Data Availability

The data that support the findings of this study are available from the corresponding author upon

reasonable request.

ACKNOWLEDGMENTS

The DNP experiments were performed under the RCNP project "Development of polarized target for new physics search via T-violation" and RCNP Collaboration Research Network program (Project No. COREnet-026) of the Research Center of Nuclear Physics, Osaka University. The material research was performed under the GIMRT Program of the Institute for Materials Research, Tohoku University (Proposal No. 19K0081, 20K0018, and 20N0002). The EPR experiments were conducted with H. Mino, Nagoya University. We would like to thank Editage (www.editage.jp) for English language editing.

REFERENCES

- ¹C. S. Wu, E. Ambler, R. W. Hayward, D. D. Hoppes, and R. P. Hudson, "Experimental test of parity conservation in beta decay," *Phys. Rev.* **105**, 1413–1415 (1957).
- ²G. Mitchell, J. Bowman, S. Penttilä, and E. Sharapov, "Parity violation in compound nuclei: experimental methods and recent results," *Phys. Rep.* **354**, 157–241 (2001).
- ³V. Gudkov, "On CP violation in nuclear reactions," *Phys. Rep.* **212**, 77–105 (1992).
- ⁴T. Okudaira, S. Takada, K. Hirota, A. Kimura, M. Kitaguchi, J. Koga, K. Nagamoto, T. Nakao, A. Okada, K. Sakai, H. M. Shimizu, T. Yamamoto, and T. Yoshioka, "Angular distribution of γ rays from neutron-induced compound states of ^{140}La ," *Phys. Rev. C* **97**, 034622 (2018).
- ⁵T. Yamamoto, T. Okudaira, S. Endo, H. Fujioka, K. Hirota, T. Ino, K. Ishizaki, A. Kimura, M. Kitaguchi, J. Koga, S. Makise, Y. Niinomi, T. Oku, K. Sakai, T. Shima, H. M. Shimizu, S. Takada, Y. Tani, H. Yoshikawa, and T. Yoshioka, "Transverse asymmetry of γ rays from neutron-induced compound states of ^{140}La ," *Phys. Rev. C* **101**, 064624 (2020).
- ⁶Y. Takahashi, H. Shimizu, and T. Yabuzaki, "Possible nuclear polarization of ^{139}La in $\text{Nd}^{3+}:\text{LaAlO}_3$ for the test of time reversal invariance," *Nucl. Instrum. Methods Phys. Res., Sect. A* **336**, 583–586 (1993).
- ⁷T. Maekawa, Y. Takahashi, H. M. Shimizu, M. Iinuma, A. Masaike, and T. Yabuzaki, "A large nuclear polarization of ^{139}La in $\text{Nd}^{3+}:\text{LaAlO}_3$ for testing the time reversal invariance," *Nucl. Instrum. Methods Phys. Res., Sect. A* **366**, 115–119 (1995).

- ⁸P. Hautle and M. Iinuma, “Dynamic nuclear polarization in crystals of Nd³⁺:LaAlO₃, a polarized ¹³⁹La target for a test of time-reversal invariance,” *Nucl. Instrum. Methods Phys. Res., Sect. A* **440**, 638–642 (2000).
- ⁹F. Homer and C. Brandle, “Czochralski growth and detwinning of LaAlO₃,” in *Crystal growth : proceedings of an International Conference on Crystal Growth, Boston, 20-24 June 1966* (Pergamon Press, Hoboken, NJ, USA, 1967) pp. 51–55.
- ¹⁰X. Zeng, L. Zhang, G. Zhao, J. Xu, Y. Hang, H. Pang, M. Y. Jie, C. Yan, and X. He, “Crystal growth and optical properties of LaAlO₃ and Ce-doped LaAlO₃ single crystals,” *J. Cryst. Growth* **271**, 319–324 (2004).
- ¹¹R. E. Fahey, A. J. Strauss, and A. C. Anderson, “Vertical gradient-freeze growth of aluminate crystals,” *J. Cryst. Growth* **128**, 672–679 (1993).
- ¹²S. Suzuki, H. Ohsato, K.-I. Kakimoto, T. Shimada, K. Sasaki, and H. Saka, “Growth of LaAlO₃ single crystal by floating zone method and its microwave properties,” in *Advances in Electronic Ceramic Materials: Ceramic Engineering and Science Proceedings, Volume 26, Number 5* (John Wiley & Sons, Inc., Hoboken, NJ, USA, 2005) pp. 177–184.
- ¹³Y. Inagaki, S. Suzuki, I. Kagomiya, K. Kakimoto, H. Ohsato, K. Sasaki, K. Kuroda, and T. Shimada, “Crystal structure and microwave dielectric properties of SrTiO₃ doped LaAlO₃ single crystal grown by FZ,” *Journal of the European Ceramic Society* **27**, 2861–2864 (2007).
- ¹⁴J. G. Bednorz and H. Arend, “A 1 kW mirror furnace for growth of refractory oxide single crystals by a floating-zone technique,” *J. Cryst. Growth* **67**, 660–662 (1984).
- ¹⁵K. Ishizaki, H. M. Shimizu, M. Kitaguchi, T. Matsushita, M. Iinuma, H. Kohri, H. Yoshikawa, M. Yosoi, T. Shima, T. Iwata, Y. Miyachi, S. Ishimoto, M. Fujita, and Y. Ikeda, “Polarized Lanthanum Target for the T-violation Search in Slow Neutron Transmission,” *PoS PSTP2019*, 061 (2020).
- ¹⁶S. A. Hayward, F. D. Morrison, S. A. T. Redfern, E. K. H. Salje, J. F. Scott, K. S. Knight, S. Tarantino, A. M. Glazer, V. Shuvaeva, P. Daniel, M. Zhang, and M. A. Carpenter, “Transformation processes in LaAlO₃: Neutron diffraction, dielectric, thermal, optical, and raman studies,” *Phys. Rev. B* **72**, 054110 (2005).
- ¹⁷G. Court, D. Gifford, P. Harrison, W. Heyes, and M. Houlden, “A high precision Q-meter for the measurement of proton polarization in polarised targets,” *Nucl. Instrum. Methods Phys. Res., Sect. A* **324**, 433–440 (1993).
- ¹⁸I. Ide, M. Fujita, H. Hotta, M. Iinuma, Y. Ikeda, Y. Ito, T. Iwata, M. Kitaguchi, H. Kohri,

D. Miura, Y. Miyachi, T. Okudaira, H. M. Shimizu, Y. Takanashi, and M. Yosoi, “Current status of polarized La target development for T-violation search with slow neutron,” PoS **PSTP2022**, 038 (2023).